8-2011

Synthesis and Characterization of N- and P- Doped Tin Oxide Nanowires

Hoang Tran
Portland State University

Shankar B. Rananavare
Portland State University, ranavas@pdx.edu

Synthesis and Characterization of N- and P- Doped Tin Oxide Nanowires

Hoang A. Tran and Shankar B. Rananavare

Abstract— **Bulk-scale synthetic methods for preparing doped tin oxide (SnO_2) nanowires (NWs) are presented. n-and p-doping is achieved through insertion of Antimony and Lithium in tin oxide lattice, respectively. We also present a comparison of the structural and optical properties of SnO_2 nanoparticles (NPs), and SnO_2 NWs. Both n-type and p- type NWs display a characteristic red shift in their photoluminescence (PL) spectra. Surface plasmons observed in these systems imply high carrier concentrations. These corrosion resistant materials are useful in fabricating ultra-sensitive gas detectors and transparent electronics**.

Index Terms: Tin Oxide Nanowires, doped nanowires, wide band gap semiconductors, transparent oxides.

I. INTRODUCTION

1D nanostructure materials have attracted great attention in recent years [1-3] as they provide interesting possibilities for resistance-less transport due to quantum effects. Varieties of synthetic methods have been utilized to synthesize 1D nanomaterials. A most common method is based on vapor-liquid-solid (VLS) mechanism that can be carried out in a chemical vapor deposition (CVD) reactor. VLS is considered to be one of the best method for producing single crystal NWs and nanotubes in relatively large quantities [4, 5]. An adaptation of the VLS method involving solution-liquid-solid phases is developed by Buhro et al [6]. A similar solvothermal method uses solvents under very specific conditions of pressure and temperature to increase solubility of solids and speeds reactions [7] that leads to formation of NWs. Solution state methods involving templating by combination of surfactants that preferentially cap the sidewalls of growing NWs have also been developed for synthesis of metallic NWs of gold, silver etc[8, 9]. This paper focuses on solution state syntheses of doped SnO_2 NWs.

A key benefit of tin oxide over other contemporary semiconductors such as silicon or gallium arsenide is that it is a chemically stable material that is corrosion resistant. Thus, this wide band gap semiconductor (3.56eV) finds wide-ranging applications in nanoelectronics as a transparent conductor [10-13], in chemistry as heterogeneous catalysts [14-19] and also as a solid state gas sensor [20-25]. In a series of papers we have illustrated synthesis[26], characterization[26] and applications [22, 27] of NPs of SnO_2. Using compressed powders of n-doped and p-doped SnO_2 NP,S we have been able to fabricate homo-junction diode sensors capable of detecting 100ppn level of toxic oxidizing gas chlorine. One key limitation of these sensors arises from poor electron transport across the NP powders. This is a result of interparticle depletion barrier and the effects of coulomb blockade at each physical contact. Practically this limits the dynamic range of devices confining them to low concentration (below 20ppm) of the analyte. A simple method to minimize these interparticle electron/hole hops is through the replacement of NPS with aligned NWs. The resistance for transport along the single crystal nanowire is lower due to favorable quantum effects in 1-D systems[28]. Studies of electron transport through CNTs and SiNWs indicate extraordinary high mobility in these 1-D quantum fluids[29, 30].

Our goal here is to present synthetic methods for synthesizing doped NWs for tin oxide. Current methods far for the synthesis of 1D nanostructures of undoped SnO_2 include laser ablation [31, 32], molten salt [33, 34], solvo-thermal and hydrothermal methods [35, 36], thermal evaporation [37, 38], carbothermal reduction [39, 40], and rapid oxidation [41]. Herein, we describe the synthesis of doped SnO_2 NWs adopting and modifying the strategy of Yang and Lee [33]. It has enabled us to synthesize n-type, antimony doped SnO_2 NWs. We introduce the first synthesis of p-doped SnO_2 1D nanostructure using lithium ion as a dopant. The latter is developed based on our current understanding of p-doped SnO_2 NPs [26, 42, 43].

II. PROCEDURE

Materials: The following chemicals were used without further purification: $SnCl_4 \cdot 5H_2O$ (>98%, Fischer Scientific), 1,10-phenanthroline monohydrate (ACS reagent, puriss. p.a., ≥99.5%, Sigma Aldrich) $NaBH_4$ (98%, Sigma Aldrich), LiCl , KCl and NaCl (>95%, Fischer Scientific). Deionized water was purified by distillation

Material characterizations: SEM data were collected on a FEI Sirion FEG SEM operating at 5KV with the working distance 5mm. TEM data were collected using Holey carbon TEM grids on a FEI Tecnai F-20 microscope operating at 200 kV. The optical photoluminescence (PL) of the doped and undoped SnO_2 NWs was characterized on a Shimadzu spectrofluorophotometer RF-5301PC, using a xenon light source and 3nm bandwidth. As-prepared samples including NPs and NWs were dispersed in water for the PL measurements. Fourier transform infra red (FTIR) spectra were acquired on a Perkin-Elmer RXI instrument. For Infra-red as well as UV-visible-NIR (Shimadzu UV 3600) spectroscopic investigations, samples consisted of solid powders sandwiched between quartz plates. This protocol is

Hoang Tran is with Department of Chemistry, Portland State University; Portland OR 97027 USA; (e-mail: hoangt@ pdx.edu).

Shankar Rananavare is with Department of Chemistry, Portland State University; Portland OR 97027 USA; (e-mail: ranavas@ pdx.edu).

different from the commonly used, solvent dispersed studies of these materials.

Synthetic methods:

n-doped tin oxide NWs: The precursors Sn NPs were synthesized by reducing a thoroughly mixed solution of 50 ml of 0.05 M $SnCl_4 \cdot 5H_2O$ and 0.5 g of 1,10-phenanthroline with 100ml of 0.1 M $NaBH_4$ aqueous solution. The reducing solution was introduced drop wise to synthesize phenanthroline capped Sn nanoparticles [44]. NPs were separated from the reaction mixture by centrifuging (10,000 rpm for 15 minutes) after two hours of reaction time. The precipitate was dried at 50ºC in 2hrs on a hotplate. 0.2 g of 1,10-phenanthroline capped Sn NP powder was mixed with a mixture of 0.4 g of NaCl and 0.6 g of KCl, grounded into a fine powder, and heated at 750 °C for 2 h in a furnace. The molten mixture was then slowly cooled to room temperature. The solidified product was washed several times with water, to remove KCl and NaCl. Their removal was tested with 0.05mM $AgNO_3$ solution for any residual Cl$^-$ anion. The wet powder was dried in an over at 100°C overnight to remove water. For n-doping, varying amount of antimony chloride (1-5% at. wt. in relation to Sn) was added to the initial solution of $SnCl_4 \cdot 5H_2O$ and 1,10-phenanthroline. The rest of the synthetic procedure was identical to the synthesis of undoped NWs as described above. Note that the actual amount of dopant inserted in NPs could be different than the concentration of dopant atoms used during synthesis.

P-doped tin oxide NWs: For p-doping, LiCl replaced antimony chloride as a dopant. The amounts of lithium chloride added to the initial reaction mixture ranged from 1 to 5 wt%. The precursors Sn NPs coated with a thin layer of tin oxide were synthesized without capping agents by adding 0.35g $SnCl_4 \cdot 5H_2O$ with 0.1 M $NaBH_4$ aqueous solution containing LiCl. The mixture turned black, indicating the formation of oxide coated Sn NPs. The precipitate was collected by filtering and was left to dry in air over night. 0.2g of the above precursor was mixed with 0.2g of1,10-phenanthroline, 0.31g of LiCl and 0.6g of KCl, grounded into a fine powder, and was kept at 480^{0}C for 2hr. The molten mixture was then slowly cooled to room temperature with cooling rate of 4^{0}C/minute. The product was collected and purified as in the case of undoped NWs.

III. RESULTS AND DISCUSSION

The morphology of as-prepared un-doped and Sb-doped SnO_2 NWs was characterized by SEM; see figure 1. The majority of the un-doped NWs showed an average NW diameter ranging from 20 to 50 nms and the length up to micron. This morphology was mixed with a whisker-like nanorods. In n-doped NWs, the size distribution was much broader, perhaps due to incorporation and morphological effects of dopant atoms (but see below). Also, note that the smaller diameter NWs tended to fuse with one other. Since such structures are rarely observed in the nucleation and growth of NWs mediated by the VLS mechanism, the mechanism of growth of these NWs is likely to be governed by the surface energy of NW walls as controlled by the

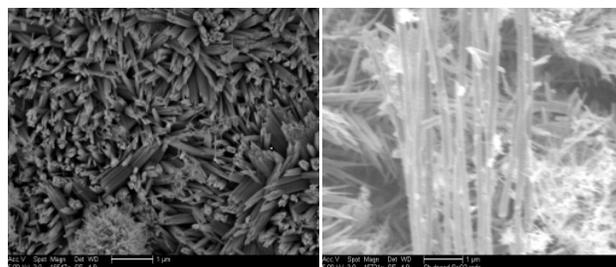capping agent phenanthroline. TEM and High resolution

Figure 1: SEM images of undoped (left) and Sb doped NWs (right)

TEM of n-doped NWs, shown in figure 2 along with electron diffraction in inset indicated single crystalline nature of NWs. The crystal structure of these 20nm diameter NWs was a characteristic cassiterite type (details are not shown here) which is commonly observed upon calcination at 500ºC in SnO_2 NPs synthesized by sol-gel method[26]. Also, it can be seen that the nanowire growth mechanism is neither VLS (no spherical catalyst droplet on the tip) or solution-liquid-solid (SLS). The NWs showed a very straight and smooth surface morphology suggesting a 1-D Ostwald-ripening mechanism [34] in which NPs deposit onto, dissolve into each other and extrude to form a 1D nanostructures.
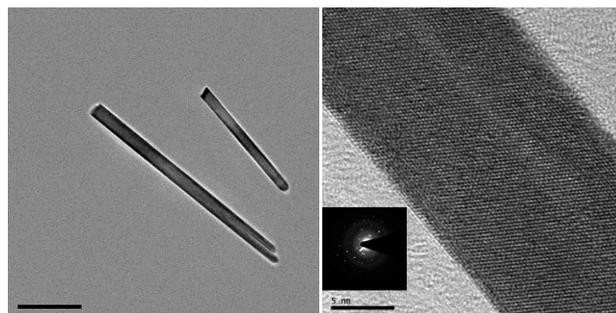

Figure 2: TEM of n-doped SnO_2 NWs with low and high magnifications.

Room-temperature photoluminescence spectra of undoped SnO_2 NPs and NWs appear in figure 3.
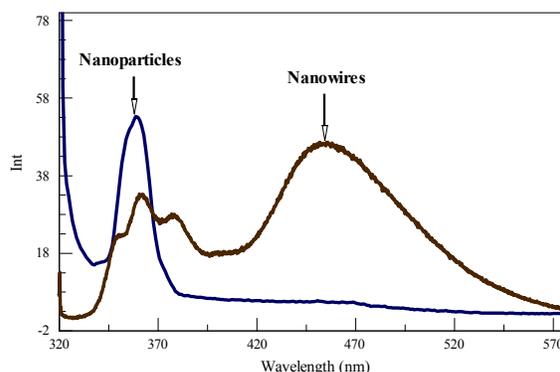

Figure 3: PL of undoped NWs and NPs (excitation wavelength 310 nm).

The excitation wavelength used in this study was 310nm corresponding to energy greater than the bulk bandgap energy for SnO_2. Two different PL characteristics were observed for NPs and NWs. Both nanostructures gave a strong UV emission at 360nm, corresponding to the band gap of SnO_2 (3.56ev) which partially overlapped with Raman scattering of water. The latter peak appears at a constant frequency difference from excitation.

Bulk SnO_2 is an indirect band-gap semiconductor so it is not expected to have a strong PL corresponding to its bandgap energy, as it would violate the principle of momentum conservation. Observation of PL in these the nanogeometries (i.e. in both NPs and NWs) implies a PL characteristic of a direct band-gap type semiconductor. Similar effects are well known in silicon NPs, porous silicon and silicon NWs [45] are not still well understood. Interestingly, the NWs have an additional broad emission peak near 460nm (2.7ev). The precise understanding of this PL peak currently does not exist; although explanations in terms defects including vacancies of oxygen, dopant segregation, and lattice disorders inside the lattice of SnO_2[34, 46-48] or near surface can be advanced.

Presence of dopant, especially in high concentrations, can lead to impurity band near the conduction (in the case of n-type dopant) or the valence (in the case of p-type dopant) bands. The resulting band gap narrowing could result in red shift in the PL. As shown in figure 4, under the same excitation wavelength 280nm, both un-doped and n-doped SnO_2 NWs gave two UV emission peaks, one, at 310 nms, is due to solvent Raman scattering and the other broad peak appears at 360nm wavelength. For the latter peak a red shift of 20nm was observed for Sb doped NWs in comparison with the undoped NWs. This is consistent with a dopant induced band-gap narrowing concept.

At this time, we do not have an adequate explanation for the disappearance 450 nm peak observed in undoped NWs when excited with 310 nm wavelength. Currently accepted interpretation of the 450 nm peak ascribed to oxygen vacancies, cannot explain the disappearance of this peak when excited by 280nm wavelength.
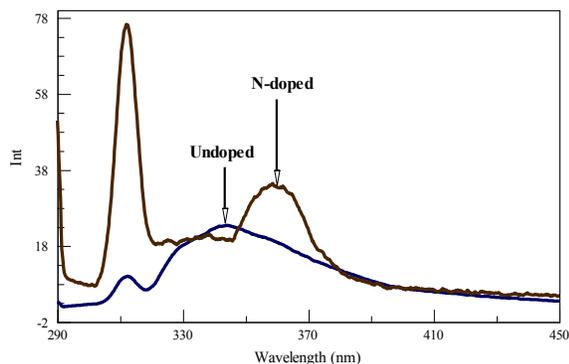
Figure 5, presents SEM images of p-doped NWs. Broad size distributions for length and diameter were observed. The length of wires varied from 200 nm up to 1 um while the diameter of single wire ranged from 50 nm to hundreds of nanometers. Like n-doped NWs, whisker-like nanorods with smaller diameters and shorter lengths were also observed along with the tendency of NWs to fuse. Thus, preformed NPs transformed into NWs through recrystallization from alkali halide salts exhibited similar characteristics regardless of the nature (n or p type) of the dopant. The morphology of NW nanostructure was influenced by a variety of factors, such as precursors, growth temperature, and the moisture content of grounded mixture before the recrystallization. The pre-synthesized powder, when dried to get rid of moisture, gave a better yield of wires and more uniform dimensional distributions. Also, the NWs formed at temperatures higher than 450ºC, gave longer wires (>1um in length) with more uniform length distribution as shown in Figure 5. Replacing coated Sn NP precursors by SnO NPs [49] did not produce NWs at 450°C. However, recrystallization at 750°C did produce NWs with low yield.
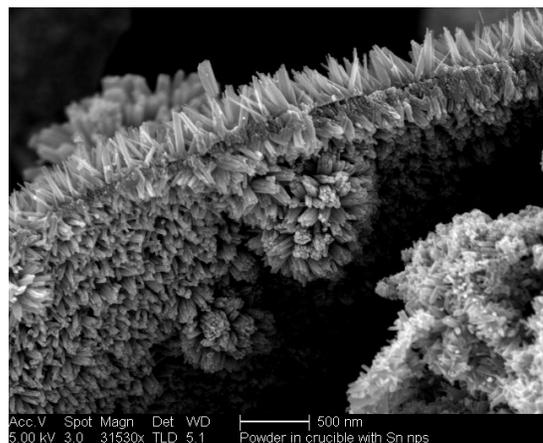

Figure 5: SEM image of p-doped SnO_2 NWs synthesized at 480°C

Single crystaline SnO coated Sn NP precursors and NWs were observed in TEM (figure 6a). NPs showed the spherical shape with mean diameter around 10 nm, and showed a tendency to agglomerate perhaps due to absence of interfacial capping agent.
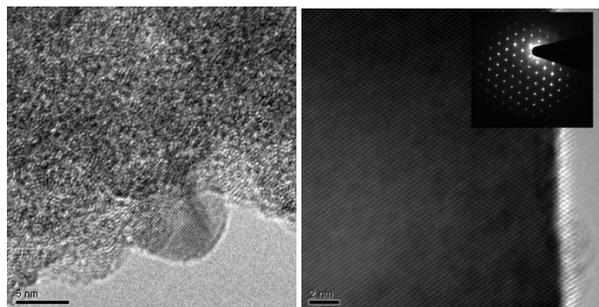

Figure 6: a) TEM of SnO_{2-x} coated Sn NP precursors and b) TEM of p-doped SnO_2 NWs

The agglomeration of NPs was perhaps responsible for the observed fused NWs during the growth process. The HR-

Figure 4: PL of un-doped and n-doped SnO_2 NWs (excitation wavelength 280 nm). The red shift of 20nm is observed.

TEM of p-doped SnO_2 NWs shown in figure 6b indicated their single crystalline nature, which was further confirmed by electron diffraction shown in the inset of figure 6b. The TEM data showed that an interplanar spacing is about 0.34 nm, which corresponds to the (110) plane of the cassiterite crystal structure of SnO_2.

A comparison of PL spectra, excited with 280nm, in undoped, 5% n- and 5% p-doped SnO_2 NWs is shown in figure 7. Two emission peaks were observed for all different types (undoped, n- and p-doped) of NWs. The first peak at 310 nm is due to solvent. The PL of p-doped NWs also showed a red shift ($\approx$25nms) for the broad emission peak occurring at 365nms.
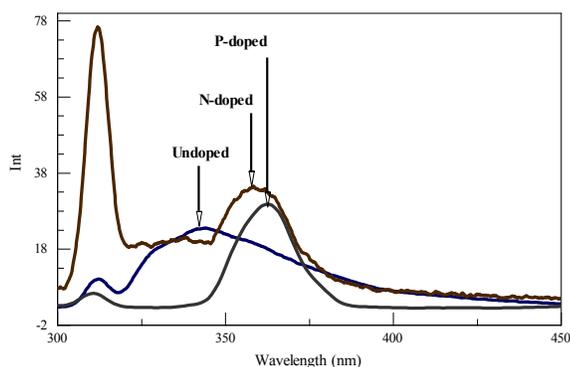

Figure 7: PL un-doped, 5% n-doped and 5% p-doped SnO_2 NWs.

Tin oxide doping was also investigated through studies of surface plasmons. For Sb-doped tin oxide NPs surface plasmons in the near IR to mid IR range were observed and carrier densities in range of $10^{20-21}cm^{-3}$ were reported[50] for 5-20% dopant concentration[1]. Our studies of n-doped NPs and Nws gave surface plasmon peaks near 2300 nm (not shown) corresponding to the carrier density of $1\times10^{21}cm^{-3}$.

UV-visible-NIR studies of p-doped NPs and NWs, shown in figure 8, suggested a shift in the surface plasmon resonance peak to the Mid-IR region reflecting a significant reduction in the carrier density. Note, that even an undoped SnO_2 tends to be an n-type semiconductor, due to the non-stoichiometric nature of the oxide, i.e., it is SnO_{2-x} and not SnO_2, where x is small but positive. The loss of oxygen deposits excess electrons in the conduction band and positively charged immobile oxygen vacancies in the crystalline lattice. Thus, to realize a p-type semiconductor, the excess electrons have be first neutralized, i.e., the Fermi level has to be pushed towards the valence band requiring significantly higher p-type dopant concentration[26, 42] to insert the equivalent hole carrier density.
To verify if the surface plasmon peak indeed appears in the

mid-IR region we collected IR spectra from the powders of NP and NWs. The data shown in figure 9, exhibited a strong peak near 3400 nm region, i.e., a clear continuation of the incipient peaks seen in the NIR spectra (figure 8). The corresponding carrier concentration was $1.6 \times10^{21}cm^{-3}$ for p-doped NPs.

The plasmon peak position for the p-doped NWs barely shifted, yet the width of the peak was clearly broader implying a shorter collisional lifetime of the carriers. This could result from relatively high surface area to volume ratios for NWs than NPs. The failure to shift the peak to lower wavelengths, i.e., lower concentration of inserted
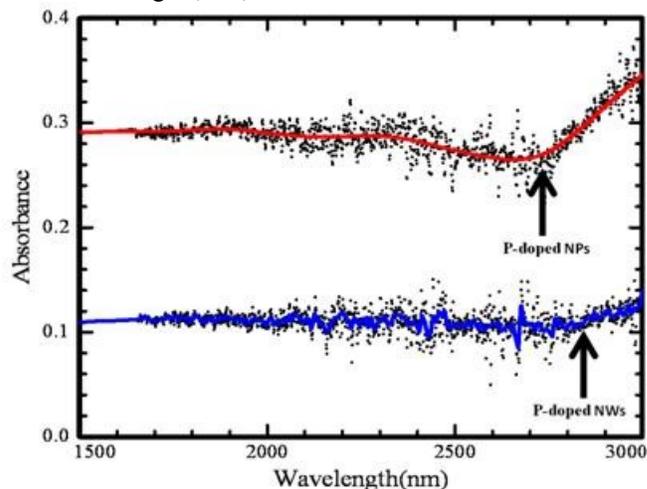

Figure 8 Optical absorption spectra for p-doped NP and NWs. The surface plasmanon peaks are just beyond the range of the instrument. Smooth lines are drawn to guide eye.

p-type dopants (even in LiCl solvent) could imply a radial concentration gradient of dopant or even formation Li_2SnO_3[27]. Further NMR studies[42] are currently underway to explore the location of the inserted Li in the NWs.
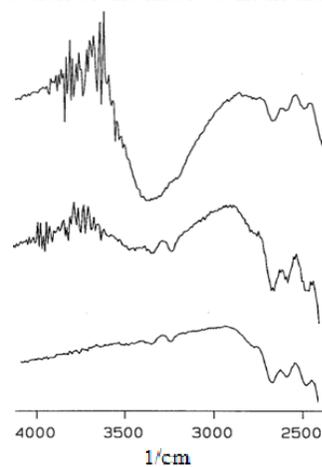
Figure 9 FTIR spectra of p-doped NPs (top), NWs (middle) and quartz substrate (bottom). The y-axis scale is transmittance and the spectra are shifted vertically for better display. Surface Plasmon wavelength for NPs is about 3400nm and the corresponding carrier density is 1.6×10^{20} cm^{-3}. The carrier density for the p-doped NWs is similar.

---

[1] These concentrations correspond to the concentration of dopants during sol-gel synthesis, which are not necessarily the actual dopant concentrations in the final NPs. Nanoscopic phase separation, compound formation etc can significantly reduce the actual dopant concentrations in the lattice.

IV. Conclusion

First synthesis of single crystalline n-doped and p-doped SnO_2 NWs is reported. These structures exhibit two strong emission bands in fluorescence spectra and display surface plasmon peaks in the Near to Mid IR regions implying a high carrier concentrations. Availability of both n- and p-type NWs opens up new opportunities for crafting transparent nanoelectronic devices, sensors etc.

Acknowledgment

References

[1] A. P. Alivisatos, "Semiconductor Clusters, Nanocrystals, and Quantum Dots," *Science,* vol. 271, pp. 933-937, February 16, 1996 1996.

[2] C. Dekker, "Carbon Nanotubes as Molecular Quantum Wires," *Physics Today,* vol. 52, pp. 22-28, 1999.

[3] J. Hu, T. W. Odom, and C. M. Lieber, "ChemInform Abstract: Chemistry and Physics in One Dimension: Synthesis and Properties of Nanowires and Nanotubes," *ChemInform,* vol. 30, pp. no-no, 1999.

[4] R. S. Wagner and W. C. Ellis, "VAPOR-LIQUID-SOLID MECHANISM OF SINGLE CRYSTAL GROWTH," *Applied Physics Letters,* vol. 4, pp. 89-90, 1964.

[5] X. Duan and C. M. Lieber, "ChemInform Abstract: Laser-Assisted Catalytic Growth of Single Crystal GaN Nanowires," *ChemInform,* vol. 31, pp. no-no, 2000.

[6] T. J. Trentler, K. M. Hickman, S. C. Goel, A. M. Viano, P. C. Gibbons, and W. E. Buhro, "Solution-Liquid-Solid Growth of Crystalline III-V Semiconductors: An Analogy to Vapor-Liquid-Solid Growth," *Science,* vol. 270, pp. 1791-1794, December 15, 1995 1995.

[7] J. R. Heath and F. K. LeGoues, "A liquid solution synthesis of single crystal germanium quantum wires," *Chemical Physics Letters,* vol. 208, pp. 263-268, 1993.

[8] F. Kim, K. Sohn, J. Wu, and J. Huang, "Chemical Synthesis of Gold Nanowires in Acidic Solutions," *Journal of the American Chemical Society,* vol. 130, pp. 14442-14443, 2008.

[9] G. Yan, L. Wang, and L. Zhang, "Recent research progress on preparation of silver nanowires by soft solution method..." *Rev. Adv. Mater. Sci.,* vol. 24, pp. 10-25, 2010.

[10] I. Hamberg and C. G. Granqvist, "Evaporated Sn-Doped In2o3 Films - Basic Optical-Properties and Applications to Energy-Efficient Windows," *Journal of Applied Physics,* vol. 60, pp. R123-R159, 1986.

[11] J. F. Wager, "Transparent Electronics," *Science,* vol. 300, pp. 1245-1246, May 23, 2003 2003.

[12] R. L. Hoffman, B. J. Norris, and J. F. Wager, "ZnO-based transparent thin-film transistors," *Applied Physics Letters,* vol. 82, pp. 733-735, 2003.

[13] R. E. Presley and et al., "Tin oxide transparent thin-film transistors," *Journal of Physics D: Applied Physics,* vol. 37, p. 2810, 2004.

[14] G. E. Batley, A. Ekstrom, and D. A. Johnson, "Studies of topochemical heterogeneous catalysis : 3. Catalysis of the reduction of metal oxides by hydrogen," *Journal of Catalysis,* vol. 34, pp. 368-375, 1974.

[15] G. Croft and M. J. Fuller, "Water-promoted oxidation of carbon monoxide over tin(IV) oxide-supported palladium," *Nature,* vol. 269, pp. 585-586, 1977.

[16] G. C. Bond, L. R. Molloy, and M. J. Fuller, "Oxidation of carbon monoxide over palladium-tin(IV) oxide catalysts: an example of spillover catalysis," *Journal of the Chemical Society, Chemical Communications,* pp. 796-797, 1975.

[17] P. G. Harrison, C. Bailey, and W. Azelee, "Modified Tin(IV) Oxide (M/SnO2M=Cr, La, Pr, Nd, Sm, Gd) Catalysts for the Oxidation of Carbon Monoxide and Propane," *Journal of Catalysis,* vol. 186, pp. 147-159, 1999.

[18] F. Solymosi and J. Kiss, "Adsorption and reduction of NO on tin(IV) oxide doped with chromium(III) oxide," *Journal of Catalysis,* vol. 54, pp. 42-51, 1978.

[19] T. Matsui, T. Okanishi, K. Fujiwara, K. Tsutsui, R. Kikuchi, T. Takeguchi, and K. Eguchi, "Effect of reduction-oxidation treatment on the catalytic activity over tin oxide supported platinum catalysts," *Science and Technology of Advanced Materials,* vol. 7, pp. 524-530, 2006.

[20] C. Cané, I. Gràcia, A. Götz, L. Fonseca, E. Lora-Tamayo, M. C. Horrillo, I. Sayago, J. I. Robla, J. Rodrigo, and J. Gutiérrez, "Detection of gases with arrays of micromachined tin oxide gas sensors," *Sensors and Actuators B: Chemical,* vol. 65, pp. 244-246, 2000.

[21] F. Allegretti, N. Buttá, L. Cinquegrani, and S. Pizzini, "A tin oxide semiconductor sensor for oxygen determination in the sub-ppm range," *Sensors and Actuators B: Chemical,* vol. 10, pp. 191-195, 1993.

[22] A. Chaparadza and S. B. Rananavare, "Room temperature Cl 2 sensing using thick nanoporous films of Sb-doped SnO 2," *Nanotechnology,* vol. 19, p. 245501, 2008.

[23] N. Buttà, L. Cinquegrani, E. Mugno, A. Tagliente, and S. Pizzini, "A family of tin oxide-based sensors with improved selectivity to methane," *Sensors and Actuators B: Chemical,* vol. 6, pp. 253-256, 1992.

[24] J. Tamaki, T. Maekawa, N. Miura, and N. Yamazoe, "CuO-SnO2 element for highly sensitive

and selective detection of H2S," *Sensors and Actuators B: Chemical,* vol. 9, pp. 197-203, 1992.

[25] J. M. Wu, "A room temperature ethanol sensor made from p-type Sb-doped SnO 2 nanowires," *Nanotechnology,* vol. 21, p. 235501, 2010.

[26] A. Chaparadza, S. B. Rananavare, and V. Shutthanandan, "Synthesis and characterization of lithium-doped tin dioxide nanocrystalline powders," *Materials Chemistry and Physics,* vol. 102, pp. 176-180, 2007.

[27] Joo C. Chan, Nicole A. Hannah, Shankar B. Rananavare, Laura Yeager, Liviu Dinescu, Ashok Saraswat, Pradeep Iyer, and J. P. Coleman, "Mechanisms of Aging of Antimony Doped Tin Oxide Based Electrochromic Devices," *The Japan Society of Applied Physics,* vol. 45, pp. L1300-L1303, 2006

[28] F. D. M. Haldane, "'Luttinger liquid theory' of one-dimensional quantum fluids. I. Properties of the Luttinger model and their extension to the general 1D interacting spinless Fermi gas," *Journal of Physics C: Solid State Physics,* vol. 14, p. 2585, 1981.

[29] T. Darkop, S. A. Getty, E. Cobas, and M. S. Fuhrer, "Extraordinary Mobility in Semiconducting Carbon Nanotubes," *Nano Letters,* vol. 4, pp. 35-39, 2003.

[30] O. Gunawan, L. Sekaric, A. Majumdar, M. Rooks, J. Appenzeller, J. W. Sleight, S. Guha, and W. Haensch, "Measurement of Carrier Mobility in Silicon Nanowires," *Nano Letters,* vol. 8, pp. 1566-1571, 2008.

[31] J. Q. Hu, Y. Bando, Q. L. Liu, and D. Golberg, "Laser-Ablation Growth and Optical Properties of Wide and Long Single-Crystal SnO2 Ribbons," *Advanced Functional Materials,* vol. 13, pp. 493-496, 2003.

[32] Z. Liu, D. Zhang, S. Han, C. Li, T. Tang, W. Jin, X. Liu, B. Lei, and C. Zhou, "Laser Ablation Synthesis and Electron Transport Studies of Tin Oxide Nanowires," *Advanced Materials,* vol. 15, pp. 1754-1757, 2003.

[33] Y. Wang and J. Y. Lee, "Molten Salt Synthesis of Tin Oxide Nanorods:â€‰ Morphological and Electrochemical Features," *The Journal of Physical Chemistry B,* vol. 108, pp. 17832-17837, 2004.

[34] W. Wang, J. Niu, and L. Ao, "Large-scale synthesis of single-crystal rutile SnO2 nanowires by oxidizing SnO nanoparticles in flux," *Journal of Crystal Growth,* vol. 310, pp. 351-355, 2008.

[35] C. Yu, J. C. Yu, F. Wang, H. Wen, and Y. Tang, "Growth of single-crystalline SnO2 nanocubes via a hydrothermal route," *CrystEngComm,* vol. 12, pp. 341-343, 2010.

[36] Z. Guifu and et al., "Solvothermal/hydrothermal route to semiconductor nanowires," *Nanotechnology,* vol. 17, p. S313, 2006.

[37] Z. W. Pan, Z. R. Dai, and Z. L. Wang, "Nanobelts of Semiconducting Oxides," *Science,* vol. 291, pp. 1947-1949, March 9, 2001 2001.

[38] H. Kim, J. Lee, and C. Lee, "Growth of tin oxide rod-like and sheet-like structures," *Journal of Materials Science: Materials in Electronics,* vol. 20, pp. 99-104, 2009.

[39] J. X. Wang, D. F. Liu, X. Q. Yan, H. J. Yuan, L. J. Ci, Z. P. Zhou, Y. Gao, L. Song, L. F. Liu, W. Y. Zhou, G. Wang, and S. S. Xie, "Growth of SnO2 nanowires with uniform branched structures," *Solid State Communications,* vol. 130, pp. 89-94, 2004.

[40] P. Nguyen, H. T. Ng, J. Kong, A. M. Cassell, R. Quinn, J. Li, J. Han, M. McNeil, and M. Meyyappan, "Epitaxial Directional Growth of Indium-Doped Tin Oxide Nanowire Arrays," *Nano Letters,* vol. 3, pp. 925-928, 2003.

[41] X. L. Ma, Y. Li, and Y. L. Zhu, "Growth mode of the SnO2 nanobelts synthesized by rapid oxidation," *Chemical Physics Letters,* vol. 376, pp. 794-798, 2003.

[42] A. Chaparadza and S. B. Rananavare, "Towards p-type conductivity in SnO 2 nanocrystals through Li doping," *Nanotechnology,* vol. 21, p. 035708, 2010.

[43] B.-M. Mohammad-Mehdi and S.-S. Mehrdad, "Electrical, optical and structural properties of Li-doped SnO 2 transparent conducting films deposited by the spray pyrolysis technique: a carrier-type conversion study," *Semiconductor Science and Technology,* vol. 19, p. 764, 2004.

[44] Y. Wang, J. Y. Lee, and T. C. Deivaraj, "Controlled Synthesis of V-shaped SnO2 Nanorods," *The Journal of Physical Chemistry B,* vol. 108, pp. 13589-13593, 2004.

[45] J. C. Chan, H. Tran, J. W. Pattison, and S. B. Rananavare, "Facile pyrolytic synthesis of silicon nanowires," *Solid-State Electronics,* vol. 54, pp. 1185-1191, 2010.

[46] T. W. Kim, D. U. Lee, and Y. S. Yoon, "Microstructural, electrical, and optical properties of SnO[sub 2] nanocrystalline thin films grown on InP (100) substrates for applications as gas sensor devices," *Journal of Applied Physics,* vol. 88, pp. 3759-3761, 2000.

[47] C. M. Liu, X. T. Zu, Q. M. Wei, and L. M. Wang, "Fabrication and characterization of wire-like SnO 2," *Journal of Physics D: Applied Physics,* vol. 39, p. 2494, 2006.

[48] B. Wang, Y. H. Yang, C. X. Wang, N. S. Xu, and G. W. Yang, "Field emission and photoluminescence of SnO[sub 2] nanograss," *Journal of Applied Physics,* vol. 98, pp. 124303-4, 2005.

[49] S. Majumdar, S. Chakraborty, P. S. Devi, and A. Sen, "Room temperature synthesis of nanocrystalline SnO through sonochemical route," *Materials Letters,* vol. 62, pp. 1249-1251, 2008.

[50] T. Nutz, U. z. Felde, and M. Haase, "Wet-chemical synthesis of doped nanoparticles: Blue-colored colloids of n-doped SnO[sub 2]:Sb," *The Journal of Chemical Physics,* vol. 110, pp. 12142-12150, 1999.